

SYNTHESIS AND CHARACTERIZATION OF ELECTRODEPOSITED NI-W ALLOYS WITH DIFFERENT LEVELS OF TUNGSTEN CONTENT

Maria POROCH-SERIȚAN¹, Gheorghe GUTT¹, Traian SEVERIN², Silviu-Gabriel STROE¹

¹„Ștefan cel Mare” University of Suceava, Faculty of Food Engineering, Str. Universitatii, no. 13, 720229, Suceava, Romania, Phone: +40 230 216147, int. 298, Fax: +40 230 520267, e-mail: mariap@usv.ro, g.gutt@usv.ro

²„Ștefan cel Mare” University of Suceava, Faculty of Mechanical Engineering, Mechatronics and Management, Str. Universitatii, no. 13, 720229, Suceava, Romania, Phone: +40 230 216147, int. 298, Fax: +40 230 523743, e-mail: severintraian@fim.usv.ro

Abstract: Tungsten alloys are known for their excellent mechanical and tribological properties. Ni-W alloys exhibit enhanced properties such as corrosion resistance, wear resistance and catalytic activity for H₂, useful in practical applications. Pure tungsten cannot be electrodeposited from aqueous electrolytes, but can be codeposited with iron group elements such as nickel to form an alloy. The objective of the current work was to study the effect of bath chemistry and current density on chemical composition, microstructure and properties of Ni-W alloys deposited from citrate-containing baths, without stirring of the bath solution on copper substrate. The investigations include characterization of complex formation by UV-VIS spectrometry. The absorption spectrum of solutions with nickel in composition is similar and it shows the presence of four peaks. The current efficiency is increased with increased concentration of Ni²⁺ ions in bath. The layer thickness of the deposition obtained in NiW-I bath is low, but increase with the current density. The homogeneous hardness of the Ni-W deposit may be attributed mainly to three factors: layer thickness, the deposition structure and deposit composition. All these three factors are current density dependent. The micrograph of NiW coating, studied by scanning electron microscopy (SEM), shows the presence of cracks on a relatively uniform surface and the electron diffraction spectroscopy (EDS) analysis confirmed that Ni and W are uniformly distributed on the surface.

Keywords: electrodeposited Ni-W alloys, current density, chemical composition, microstructure, properties

Introduction

The interest in electrodeposition of nickel-tungsten (Ni-W) alloys has increased in recent years due their excellent corrosion resistance [1], [2], [3], wear resistance, high hardness and magnetic properties [4], [5]. Lowe et al. [6] found that the hardness of Ni-W alloys is three times higher than that of pure electrodeposited Ni. In addition, the hardness is found to increase with increase in W content in the alloy as reported by Singh et al. [7].

It is well known that tungsten cannot be

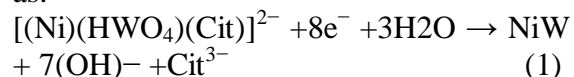
electrodeposited from an aqueous solution of sodium tungstate (Na₂WO₄) or any other soluble compound containing this element. However, if a suitable nickel compound such as nickel sulphate (NiSO₄) is added to the plating bath, induced codeposition can take place, forming Ni-W alloys. A similar phenomenon is observed during electrodeposition of W, Mo or Re with Ni, Co or Fe, as well as in electroless deposition of Ni-P or Co-P alloys.

The tungsten content of the alloy is usually in the range of 5–25 at. % (13–50 wt. %). One of the commercial plating solutions

(ENLOY® Ni-500 from Enthone), for example, yields 35–40 wt. % tungsten in the deposit [8]. In order to further improve the tribological properties and thermal stability of the coating, it is sometimes desirable to increase its tungsten content. Unfortunately, this has been found difficult, even when the WO_4^{2-} ion in solution is in large excess compared to the Ni^{2+} ion [9]. One possible way to increase the tungsten concentration in the alloy is to apply periodic current reverse pulse plating, which may also increase the throwing power and the deposition rate, as well as improve the properties of the deposit (e.g., reduce residual stresses and porosity, refine the grain size, improve wear and corrosion resistance, etc.) [10], [11].

Another route has recently been suggested by Gileadi and co-workers [9], [12], [13], [14], [15], who developed a novel plating bath for codeposition of Ni–W alloys with high tungsten content. By removing the NH_3 from the bath and using citrate ($\text{C}_6\text{H}_5\text{O}_7$)³⁻ as an addendum ligature, the tungsten content of the alloy could be increased to 50 at. % (76 wt. %). The working hypotheses in the above studies are that (a) the tungstate/citrate complex forms a complex with nickel citrate in the bulk of the solution or on the surface; (b) this ternary complex, of the type $[(\text{Ni})(\text{HWO}_4)(\text{Cit})]^{2-}$, is the precursor for the deposition of the Ni–W alloy; (c) nickel can also be deposited from its complexes with either citrate or NH_3 . The overall reaction of the ternary complex

requires eight electrons and can be written as:



In the previous work of Gileadi and co-workers, a rotating gold cylinder served as the working electrode. Such working electrodes, however, are impractical for industrial use. Furthermore, it is well known that codeposition of nickel and tungsten is very sensitive to changes in operating conditions.

The objective of the current work is to study the effect of bath chemistry and current density on chemical composition, microstructure, thickness and hardness of nickel – tungsten alloys deposited from citrate-containing baths, without stirring of the bath solution on copper substrate.

Materials and Methods

Preparation of NiW alloys

Nickel–tungsten alloys were electroplated from aqueous solutions containing $\text{NiSO}_4 \cdot 6\text{H}_2\text{O}$ (nickel sulphate hexahydrate, Sigma - Aldrich) and $\text{Na}_2\text{WO}_4 \cdot 2\text{H}_2\text{O}$ (sodium tungstate dehydrate, Sigma - Aldrich) as the electro-active species, and $\text{C}_6\text{H}_5\text{Na}_3\text{O}_7 \cdot 2\text{H}_2\text{O}$ (tri-sodium citrate dehydrate, Sigma - Aldrich) as complexing agent (Table 1). All reagents were dissolved in bi-distilled water (conductivity $3.406 \mu\text{S} \cdot \text{cm}^{-1}$). The pH was measured by means of pH/mV/°C meter from Cole Parmer and adjusted to a value of 8.0 through additions of H_2SO_4 and NaOH solutions.

Table 1.

The chemical composition of electrolytic baths for alloys Ni-W electroplating

Bath	$\text{NiSO}_4 \cdot 6\text{H}_2\text{O}$ [g·L ⁻¹]	$\text{Na}_2\text{WO}_4 \cdot 2\text{H}_2\text{O}$ [g·L ⁻¹]	$\text{C}_6\text{H}_5\text{Na}_3\text{O}_7 \cdot 2\text{H}_2\text{O}$ [g·L ⁻¹]
NiW-1	2.6286	131.944	147.00
NiW-2	13.143	131.944	147.00
NiW-3	26.286	131.944	147.00

In this work, the home made Hull electrochemical cell was used with a 250 ml capacity. The current intensity was calculated with the Hull - Mac Intyre

equation:

$$i = I(5,1019 - 5,240 \log l) \quad (1)$$

where: i - current density, [$\text{A} \cdot \text{dm}^{-2}$];

I - current intensity in cell circuit, [A];

l – distance along the cathode from the point of maximum current densities, [cm]. The cell was equipped with a cathode (made of 99.98 % purity copper) and a carbon anode. The cathode dimensions are of 8.0 cm (height), 9.8 cm (length), \square 0.1 cm (with) while the dimensions of anode were of 6.0 cm (height), \square 1.0 cm (length), \square 1.0 cm (with). The immersion surface of cathode was of 0.6 dm² and respectively the anodic immersion surface was of 0.045 dm². Before electrodeposition, the electrode surface was polished with emery paper (320–1000 grain size), then was had with distilled water, thoroughly degreased with acetone, activated with 20% H₂SO₄, washed once more with distilled water and immerse in the bath solution. The above described cell was connected with electroplating regime to the GWINSTEK GPR-1810HD power supply, having a digital control of current and voltage. For each experiment 1800 coulomb of electricity were used. The temperature of electrolyte solution was kept constant at the value of 25 °C. The electrodeposition was carried without stirring the bath solution.

Current efficiency

The plating current efficiency (CE) for deposition of each alloy was calculated according to the following equation:

$$CE = \frac{(m \cdot Ni\%) / Eq_1 + (m \cdot W\%) / Eq_2}{I \cdot t} \quad (2)$$

where: m is the deposit weight (g), Ni% and W% (wt.%) is the percent of nickel and tungstate in deposits, respectively, Eq_1 and Eq_2 is the electrochemical equivalent (g·C⁻¹) of Ni²⁺ and W⁶⁺, respectively, I is the deposition current (A), and t is the deposition time (s).

The percent of nickel and tungstate in deposit for the entire cathodic surface of Hull cell was calculated as the average of three determinations for each of the ten areas (previously the cathodic surface was divided into ten areas with different current

densities).

Characterization techniques

Absorption spectrum of electrolytes were recorded with a miniature spectrometer (HR 4000 CG-UV-NIR, Ocean Optics Inc., Dunedin, FL), using 1-cm cells. A tungsten halogen light source (UV-VIS-NIR Light Source DH-2000, Mikropack) was used for this study. The light from Light Source DH-2000 was conveyed to the sample through two optical fibres (QP400-2-SR/BX, Ocean Optics Inc., Dunedin, FL).

The morphology of the deposits after drying was observed with a scanning electron microscope (SEM, VEGA II LMU - Tescan, Czech Republic). The attached energy dispersive spectroscopy (EDS, Bruker AXS Microanalysis GmbH probe) was used to determine the approximate composition of the alloy. Each of the ten areas was measured in three different locations to confirm uniformity.

The thickness of metallic layer was measured by means of a PosiTector 6000 – DeFesko Analyzer, based on non-destructive physical method. Seven local values of cathode thickness were measured in order to determine the average thickness of metallic layer, U (μm).

The micro-hardness of metallic cover, W (HV), was measured using the Shimadzu, HMV – 2T, micro-hardness analyzer. The loading weight was of 490.3 mN.

Results and Discussion

Composition of the actual alloy Ni-W bath

Figure 1 shows a typical spectrum of reagents in the electrolyte composition of alloy Ni-W bath for three different nickel sulphate content of deposition bath in wavelength range from 300 to 1100 nm. It may be noted that the spectra obtained for solutions of 131.944 g·L⁻¹ Na₂WO₄·2H₂O and (131.944 g·L⁻¹ Na₂WO₄·2H₂O + 147 g·L⁻¹ C₂H₅Na₃O₇· 2H₂O) mixture have no absorption peaks. The absorption spectrum

of the deposition baths containing nickel: NiW-1 bath, 26.286 g·L⁻¹ NiSO₄·6H₂O, (26.286 g·L⁻¹ NiSO₄·6H₂O + 147 g·L⁻¹ C₂H₅Na₃O₇·2H₂O) mixture, NiW-2 bath, NiW-3 bath are similar and it shows the presence of four peaks in the following wavelength ranges: 350 – 450 nm, 600 – 700 nm, 700 – 750 nm and 1000 -1100 nm. The 4 absorption spectrum of Figure 1 is the specific absorption spectrum of nickel sulphate solution, which due to d-d electronic transitions the Ni²⁺ ion shows characteristic absorption bands in the visible spectral region with absorption maxima at 398.660 nm and 720 nm. For spectra of 5 and 3, 6, 7, respectively, due to presence of 147 g·L⁻¹ C₂H₅Na₃O₇·2H₂O and (147 g·L⁻¹ C₂H₅Na₃O₇·2H₂O + 131.944 g·L⁻¹ Na₂WO₄·2H₂O) mixture,

respectively in the electrolyte distinct changes in the Ni(II) absorption spectrum can be observed. The higher absorption values at all wavelengths due to complex formation of Ni²⁺ ions with tri-sodium citrate dehydrate or mixture of tri-sodium citrate dehydrate and sodium tungstate dehydrate have also been described in the literature [16]. It was reported [17] that at pH 4.5 nickel citrate complexes, as well as uncomplexed nickel ions (NiH₂Cit⁺, NiHCit, NiCit⁻), all coexist. The most predominant species is a mixture of NiH₂Cit⁺ and NiHCit. On the other hand, tungstate forms soluble complexes with citrate ions and at pH 4.5 the chemistry of tungstate ions is rather complex. Poly-ions are formed and it is not clear how these poly-ions interact with citrate.

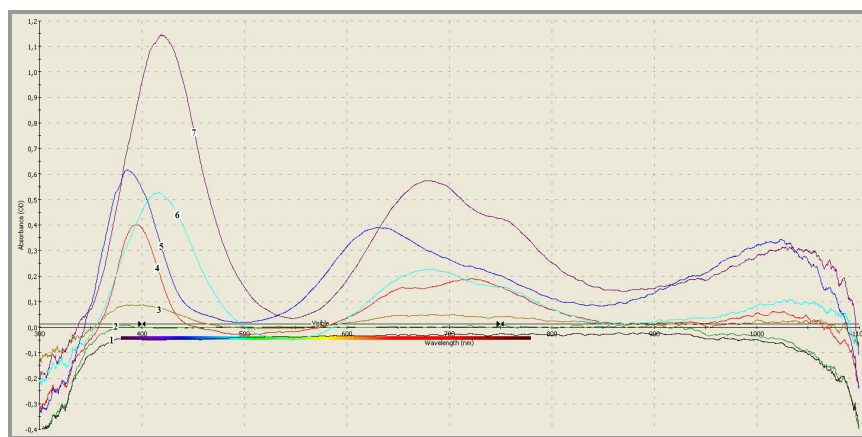


Figure 1. Overlapping spectra of UV - VIS - NIR range for the following solutions: 1 – 131.944 g·L⁻¹ Na₂WO₄ · 2H₂O, 2 – 131.944 g·L⁻¹ Na₂WO₄ · 2H₂O + 147 g·L⁻¹ C₂H₅Na₃O₇ · 2H₂O, 3 – NiW-1 bath, 4 – 26.286 g·L⁻¹ NiSO₄ · 6H₂O, 5 – 26.286 g·L⁻¹ NiSO₄ · 6H₂O + 147 g·L⁻¹ C₂H₅Na₃O₇ · 2H₂O, 6 – NiW-2 bath, 7 – NiW-3 bath

Nevertheless the equilibrium constants of different complexes of tungstate with citrate, of the type [(WO₄)(H)_n(Cit)]⁵⁻ⁿ are given in the literature and, at pH 4.5, the complex with n=2 is predominant. This is confirmed by the recent data published by Younes et al. [9] who studied the abundance of [(WO₄)(H)_n(Cit)]⁵⁻ⁿ complexes as a function of pH (in the range of 2.0–12.0). This result confirms the increase in W% with increasing pH. The tungsten can only be codeposited (together with nickel) from this ternary complex.

The existence of a ternary complex containing nickel and tungsten explains the observation that, although W is only deposited with Ni (by discharge of the ternary complex), a parallel route for deposition of Ni from its complex with citrate exists, leading to high Ni-content in the alloy.

Cathodic current efficiency and composition of Ni–W alloys

In most cases studied the cathodic current efficiency (CE) of Ni–W alloys

codeposited from citrate-containing baths is less than 100% denoting simultaneous hydrogen evolution. The effect of bath composition on the overall cathodic current efficiency for the alloy deposition as well as on the tungsten content in the deposits W% (wt. %) were analyzed and the results are given in Figure 2.

Figure 2 illustrates the influence of increasing Ni^{2+} ion content in the bath on the cathodic current efficiency of the alloy codeposition as well as on W% in the

deposit. In all cases the concentrations of the sodium tungstate dehydrate and tri-sodium citrate dehydrate in the bath were $131.944 \text{ g}\cdot\text{L}^{-1}$ and $147.00 \text{ g}\cdot\text{L}^{-1}$, respectively. At low Ni^{2+} ion concentration, the W% in the deposit is low (about 8%); however, with further increase in Ni^{2+} ion concentration, the W content in the deposit increases and reaches a maximum value of about 12%. This confirms the induced codeposition of W in the presence of Ni.

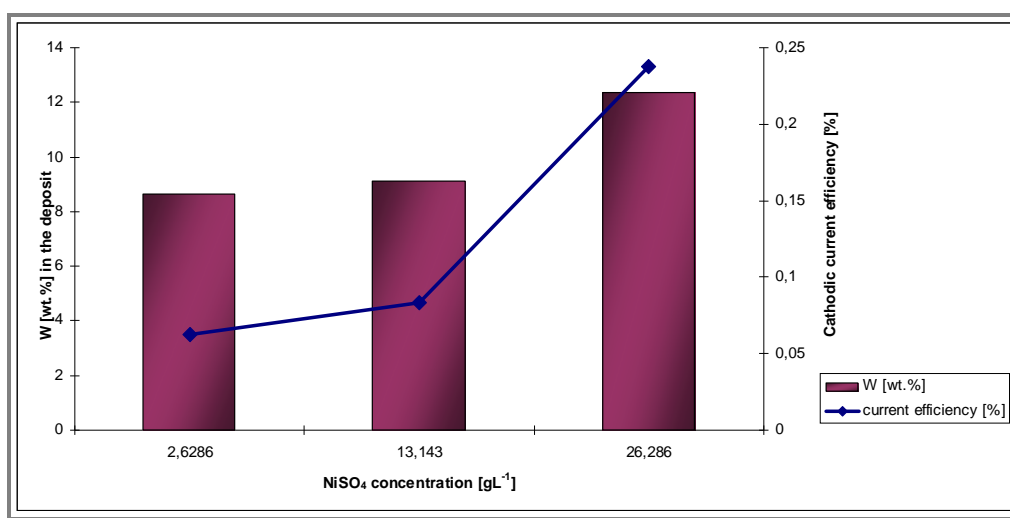


Figure 2. Effect of NiSO_4 concentration on the CE% and on W% of Ni–W alloy codeposited from NiW solution ($I=1 \text{ A}$, $\text{pH} = 8$, $t = 30 \text{ min.}$, $25 \text{ }^\circ\text{C}$).

For comparison, Younes and Gileadi [9] reported a maximum cathodic current efficiency of 11% and a maximal tungsten content of approximate 67 at. % in two different baths containing different concentrations of Na_2WO_4 . An increase in the bath concentration of Ni^{2+} has also been reported to cause a dramatic increase in the CE [13, 18]. Furthermore, it has been reported that an increase in the concentration of Ni^{2+} results in an increase in the rate of both Ni and W deposition [19, 20], but the tungsten content in the alloy decreases [15].

The effect of current density on composition of Ni–W alloys and on deposit properties

For investigating the effect of current density on the composition of Ni–W alloys from citrate-containing baths at pH of 8, the Hull cell test was carried out. The results on the appearance of deposits are shown in Figure 3. For the NiW-1 bath, zones marked with 1 and 2, zones with low current density (0 and $0.1 \text{ A}\cdot\text{dm}^{-2}$ respectively), don't have any deposition. The depositions achieved in NiW-2 bath and NiW-3 are shiny for the all density current range from 0 to $5.10 \text{ A}\cdot\text{dm}^{-2}$.

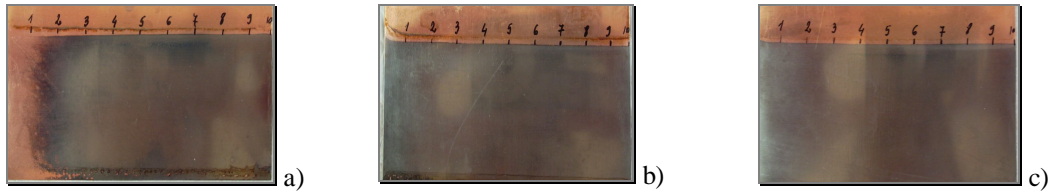


Figure 3. The appearance of Hull cell panels plated from following baths for alloys Ni-W electroplating: a) NiW-1 bath, b) NiW-2 bath, c) NiW-3 bath ($I=1$ A, $pH = 8$, $t = 30$ min., 25 °C)

Figure 4 illustrates the influence of applied current density on the thickness and on the W content in the deposit. The layer thickness of the deposition obtained in NiW-1 bath is extremely low ($0.25 \mu\text{m}$), but constant. For the NiW-2 and NiW-3 baths, the deposition layer thickness increase with the current density till $1.5 \mu\text{m}$ and $2.00 \mu\text{m}$ respectively.

Tungsten content of the deposits is influenced by the current density (Figure 4). For the deposit obtained in Ni-W-1 bath it can be observed that the tungsten content slightly increases with the current density increases. A different behaviour could be observed for the depositions achieved in NiW-2 and NiW-3 baths, where the highest W content is obtained for the lower current

density.

The effect of current density in the Ni-W system has already been studied in the literature. Brenner et al. [21] observed a significant increase in tungsten content with increasing current density in ammonia-citrate bath. Yamasaki et al. [22] reported a similar trend. Atanassov et al. [23] noted a linear increase in tungsten content with increasing current density when vigorous stirring was applied. On the other hand, a maximum was observed at $50 - 70 \text{ mA}\cdot\text{cm}^{-2}$ in the absence of stirring. At current densities higher than $20 \text{ mA}\cdot\text{cm}^{-2}$, the CE was 15 – 40% higher in the stirred bath, where hydrogen evolution was less pronounced, compared to an unstirred bath

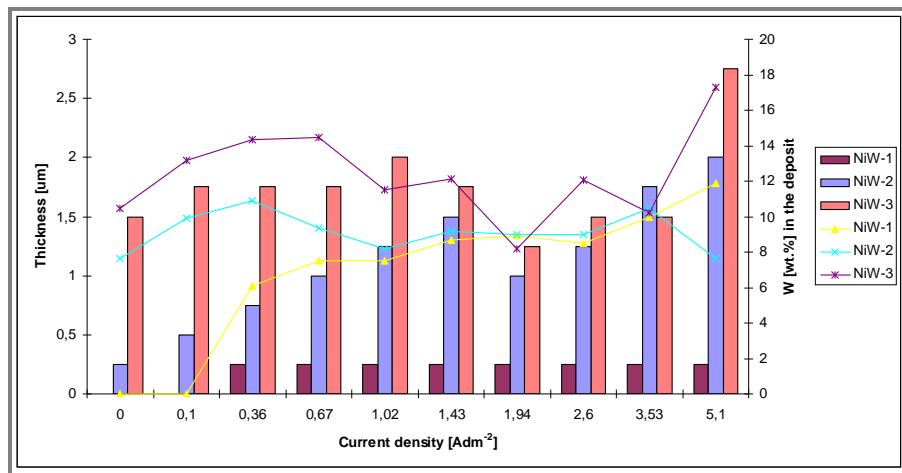


Figure 4. The influence of current density on thickness and the W content in the deposit of NiW alloy

Figure 5 represents hardness as a function of the current. The Vickers hardness of as-deposited layer is about HV98. The homogeneous hardness of the Ni-W deposit may be attributed mainly to three

factors: layer thickness, deposit structure and composition. All these three factors are current density dependent. Higher the W content and the layer thickness are, higher the deposit hardness is [24].

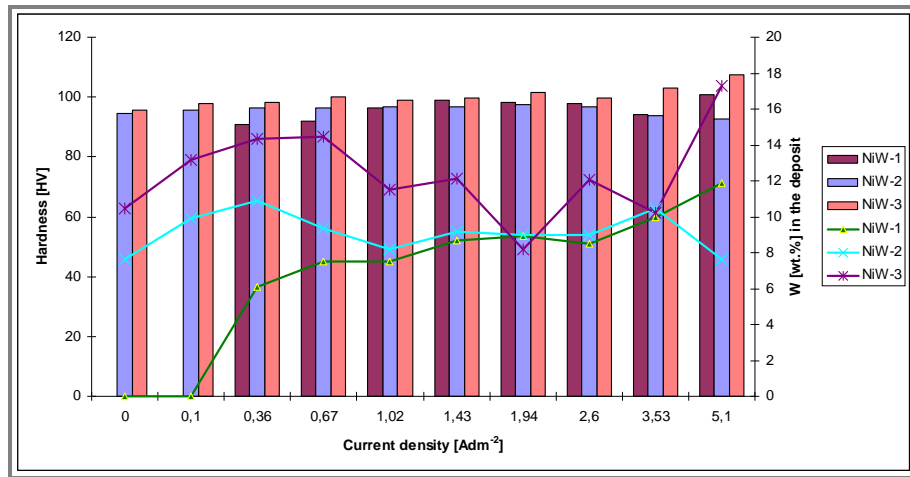
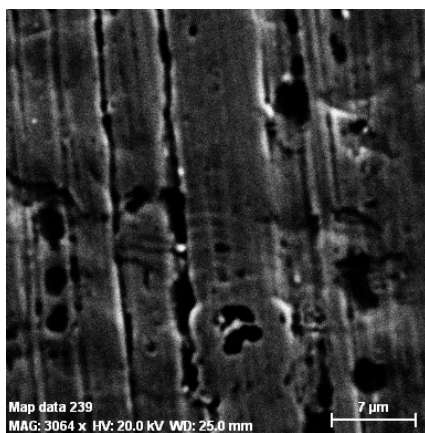


Figure 5. The influence of current density on hardness and the W content in the deposit of NiW alloy

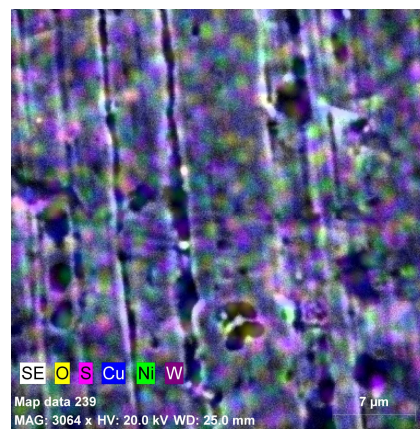
Surface morphology

The surface morphology of the as-deposited samples and their approximate chemical composition were studied by

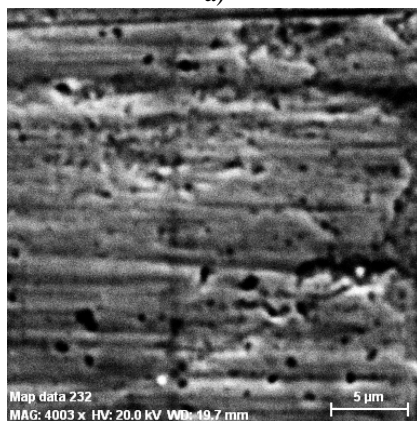
SEM and EDS, respectively. Figure 6 presents typical SEM images.



a)



b)



c)



d)

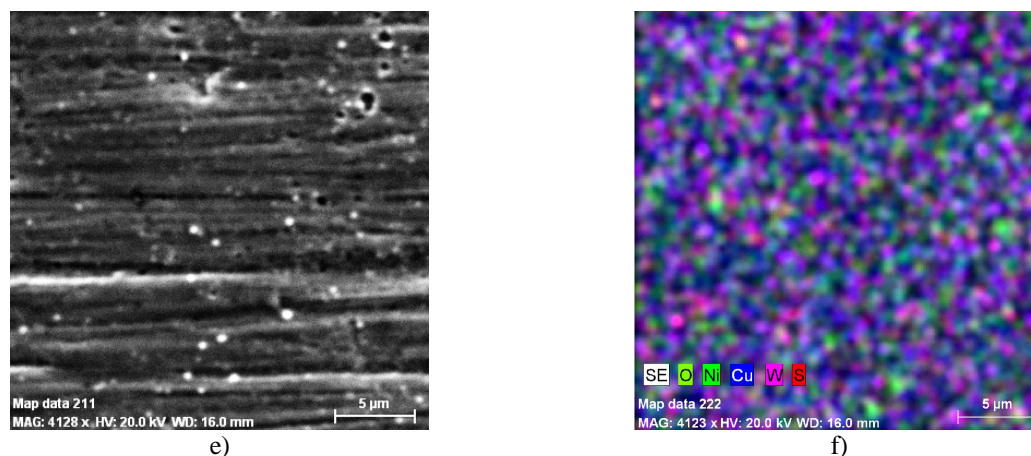


Figure 6. Scanning electron microscope secondary electron images and surface mapping images for NiW coatings in: a) - b) NiW-1 bath, $i = 1.43 \text{ A}\cdot\text{dm}^{-1}$, pH = 8, $t = 30 \text{ min.}$, 25 °C, c) - d) NiW-2 bath, $i = 3.53 \text{ A}\cdot\text{dm}^{-1}$, pH = 8, $t = 30 \text{ min.}$, 25 °C, e) - f) NiW-3 bath, $i = 5.10 \text{ A}\cdot\text{dm}^{-1}$, pH = 8, $t = 30 \text{ min.}$, 25 °C

The micrograph of NiW coating (Figures 6a, c, e) shows the presence of cracks on a relatively uniform surface, and no grains of any type could be observed even at high magnifications. Because the deposited layer is very thin, the final deposit will follow the rugosity and the surface defects of the original substrate.

Energy dispersive spectrometry (EDS) was further used in order to determine the chemical composition of the coatings and to investigate the distribution of the elements on the deposition surface (graphs are not shown here). All the EDS spectra showed the characteristic peaks for Ni and W elements. The surface mapping of Ni and W confirmed a very uniform distribution of the elements on the surfaces of all the coatings.

Conclusions

The following conclusions were drawn and discussed with respect to a comprehensive literature survey on electrodeposition of Ni–W alloys:

1) The absorption spectrum of Ni containing solutions: NiW-1 bath, 26.286 $\text{g}\cdot\text{L}^{-1}$ $\text{NiSO}_4\cdot 6\text{H}_2\text{O}$, (26.286 $\text{g}\cdot\text{L}^{-1}$ $\text{NiSO}_4\cdot 6\text{H}_2\text{O}$ + 147 $\text{g}\cdot\text{L}^{-1}$ $\text{C}_2\text{H}_5\text{Na}_3\text{O}_7 \cdot 2\text{H}_2\text{O}$) mixture, NiW-2 bath, NiW-3 bath are similar and it shows the presence of

four peaks corresponding to the wavelength ranges: 350 – 450 nm, 600 – 700 nm, 700 – 750 nm and 1000 -1100 nm.

2) The current efficiency is increased with increased concentration of Ni^{2+} ions in bath.

3) The layer thickness of the deposition obtained in NiW-1 bath is extremely low (0.25 µm), but constant. For the NiW-2 and NiW-3 baths, the deposition layer thicknesses increase with the current density till 1.5 µm and 2.00 µm respectively for a 5.10 $\text{A}\cdot\text{dm}^{-2}$ current density.

4) The homogeneous hardness of the Ni-W deposit may be attributed mainly to three factors: layer thickness, the deposition structure and deposit composition. All these three factors are current density dependent.

5) The micrograph of NiW coating shows the presence of cracks on a relatively uniform surface and the electron diffraction spectroscopy (EDS) analysis confirmed that Ni and W are uniformly distributed on the surface.

References

1. M. Obradovic, J. Stevanovic, A. Despic, R. Stevanovic and J. Stoch, *J. Serb. Chem. Soc.* 66 (2001) 899.
2. M. Obradovic, J. Stevanovic, A.R. Despic and R. Stevanovic, *J. Serb. Chem. Soc.* 64 (1999) 245.

3. D.R. Gabe, *J. Appl. Electrochem.* 27 (1997) 908.
4. T. Yamasaki, P. Schlossmacher, K. Ehrlich and Y. Ogino, *Nano-Struct. Mater.* 10 (1998) 375.
5. T. Yamasaki, *Scripta Materialia* 44(8–9) (2001) 1497.
6. H. Lowe, W. Ehrfeld and J. Diebel, *Proc. SPIE* 3223 (1997) 168.
7. V.B. Singh, L.C. Singh and P.K. Tikoo, *J. Electrochem. Soc.* 127 (1980) 590.
8. PWA 36975: Electroplated NiW—thin deposit (Enloy Ni-500). <http://www.enthone.com>.
9. O. Younes, E. Gileadi, *Electrochem. Solid-State Lett.* 3 (12) (2000) 543.
10. L. Namburi, *Electrodeposition of NiW Alloys into Deep Recess*, M.Sc. Thesis, Louisiana State University, December 2001.
11. M. Donten, Z. Stojek, H. Cesiulis, *J. Electrochem. Soc.* 150 (2) (2003) 95.
12. - O. Younes, L. Zhu, Y. Rosenberg, Y. Shacham-Diamand, E. Gileadi, *Langmuir* 17 (2001) 8270.
13. O. Younes, E. Gileadi, *J. Electrochem. Soc.* 149 (2) (2002) 100.
14. L. Zhu, O. Younes, N. Ashkenasy, Y. Shacham-Diamand, E. Gileadi, *Appl. Surf. Sci.* 200 (1–4) (2002) 1.
15. O. Younes-Metzler, L. Zhu, E. Gileadi, *Electrochim. Acta* 48 (18) (2003) 2551.
16. J. Aikaitė, O. Gylienė, O. Nivinskienė, *Formation of insoluble polynuclear Ni(II)-citrate complexes in alkaline solutions*, *Chemija* (Vilnius), 2003, T. 14, Nr.3.
17. M.A.M. Ibrahim, S.S. Abd El Rehim, S.M. Abd El Wahaab and M.M. Dankeria, *Plat. Surf. Finish.* 86 (1999) 69.
18. H. Cesiulis, A. Baltutiene, M. Donten, M.L. Donten, Z. Stojek, *J. Solid State Electrochem.* 6 (4) (2002) 237.
19. M. Donten, Z. Stojek, H. Cesiulis, *J. Electrochem. Soc.* 150 (2) (2003) 95.
20. W.H. Safranek, *The Properties of Electrodeposited Metals and Alloys*, 2nd ed., American Electroplaters and Surface Finishers Society, Orlando, FL, 1986, p. 348.
21. A. Brenner, P.S. Burkhead, E. Seegmiller, *J. Res. Natl. Bur. Stand.* 39 (1947) 351.
22. T. Yamasaki, R. Tomohira, Y. Ogino, P. Schloßmacher, K. Ehrlich, *Plat. Surf. Finish.* 87 (5) (2000) 148.
23. N. Atanassov, K. Gencheva, M. Bratoeva, *Plat. Surf. Finish.* 84 (2) (1997) 67.
24. C. Firoiu, *Tehnologia proceselor electrochimice*, Editura Didactică și Pedagogică, București, 1983